

Catalysis Science & Technology

Accepted Manuscript

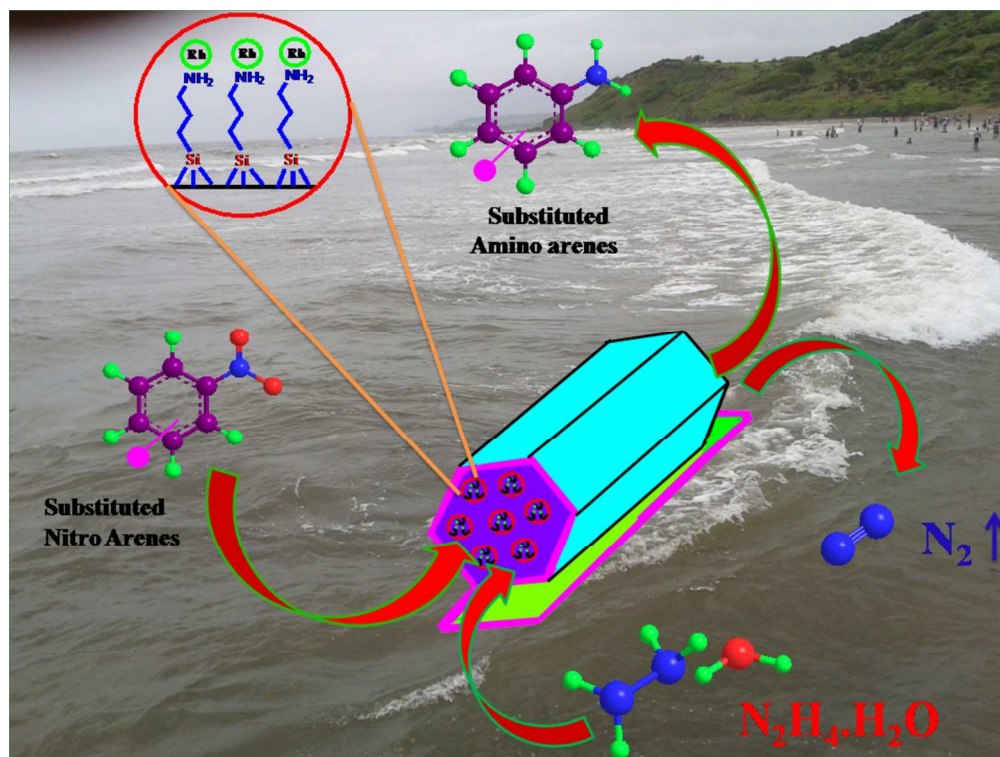


This is an *Accepted Manuscript*, which has been through the Royal Society of Chemistry peer review process and has been accepted for publication.

Accepted Manuscripts are published online shortly after acceptance, before technical editing, formatting and proof reading. Using this free service, authors can make their results available to the community, in citable form, before we publish the edited article. We will replace this *Accepted Manuscript* with the edited and formatted *Advance Article* as soon as it is available.

You can find more information about *Accepted Manuscripts* in the [Information for Authors](#).

Please note that technical editing may introduce minor changes to the text and/or graphics, which may alter content. The journal's standard [Terms & Conditions](#) and the [Ethical guidelines](#) still apply. In no event shall the Royal Society of Chemistry be held responsible for any errors or omissions in this *Accepted Manuscript* or any consequences arising from the use of any information it contains.



190x142mm (300 x 300 DPI)

RhNPs/SBA-NH₂: A high-performance catalyst for aqueous phase reduction of nitro arenes to amino arenes at room temperature

Cite this: DOI: 10.1039/x0xx00000x

Received 00th January 2012,
Accepted 00th January 2012

DOI: 10.1039/x0xx00000x

www.rsc.org/

Saidulu Ganji, Siva Sankar Enumula, Ravi Kumar Marella, Kamaraju Seetha Rama Rao and David Raju Burri*

A RhNPs/SBA-NH₂ catalyst with <3nm sized Rhodium nanoparticles has been synthesized using amine functionalized SBA-15 (SBA-NH₂) as support, rhodium acetyl acetonate as a Rh precursor and sodium borohydride (NaBH₄) as a reducing agent. RhNPs/SBA-NH₂ effectively reduced the nitroarenes to aminoarenes with nearly 100% conversion and selectivity using *in-situ* produced H₂ from hydrazine hydrate (NH₂-NH₂·H₂O) at room temperature in water medium in 5 min and the estimated turnover frequency is as high as 6117 h⁻¹ for the reduction of unsubstituted nitroarene to corresponding aminoarene.

Introduction

The reduction of nitroarenes to aminoarenes is an industrially important reaction because of the wider utility of aminoarenes in the production of pharmaceuticals, dyes, pigments and pesticides.^{1,4} Particularly, the aminoarenes are used as intermediates for the synthesis of a variety of biologically active compounds including chemo-preventive drugs, like Glu-P-1 and Trp-P-2, which can protect against several types of cancers.^{5, 6} Despite considerable amount of work is devoted for the selective reduction of nitroarenes over Pd, Pt, Ru, Rh, Au etc.,⁷⁻¹¹ some of the drawbacks like usage of environmentally harmful organic solvents, long reaction times, high temperature and high pressure operations are still preventing their potential applications.

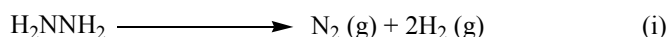
Among the principles of Green Chemistry, the use of solvents is a key aspect. However, the use of volatile organic solvents gives rise to toxic and hazardous waste. At this juncture, the use of water instead of volatile organic solvents as reaction medium is an important aspect, to gain the economical and ecological benefits^{12,13} and in addition, the time taken for heterogeneous type of organic reactions in water is dramatically shorter compared to homogeneous type of reactions, which is of great industrial importance.¹⁴

In recent years mesoporous materials have been widely used in absorption, separation and catalysis etc.¹⁵ Among them, there is an increasing interest in SBA-15 type materials as host materials for the synthesis and spatial dispersion of metal nanoparticles due to their unique properties like high surface area, uniform larger pores and high thermal stability.¹⁶ These features provide a consistent and well isolated environment for the guest molecules. Due to porous silica support characteristics agglomeration of nanoparticles gets minimized. Furthermore, the intrinsic advantages of SBA-15 supported nanoparticles catalysts are the ease of catalyst recovery and product separation.

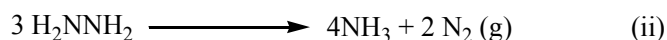
Of late, simultaneous production and utilization of hydrogen

in hydrogenation reactions has recently been emerging as a prominent area of research in heterogeneous catalysis such as transfer hydrogenation^{11a, 17}, coupling of hydrogenation and dehydrogenation reactions¹⁸, decomposition of reducing agents into H₂ and its simultaneous utilization.¹⁹ Recently, the generation of H₂ by the decomposition of hydrazine over Rh nanoparticles at room temperature has been described.²⁰ In general, the decomposition of hydrazine takes place in two pathways, which are as follows.

(i) Complete decomposition



(ii) Incomplete decomposition



Recently, Luo *et.al* reported that a Rh/PICP nanocatalyst showed efficient reduction of nitroarenes using hydrazine hydrate as reducing agent at 60 °C.²¹ In a recent report, gold nanoparticles stabilized on nano crystalline magnesium oxide actively catalyzed the selective reduction of nitroarenes with sodium borohydride in aqueous medium at room temperature²². Gao and his co workers also reported that the reduced graphene oxide catalyzed the hydrogenation of nitrobenzene at room temperature.²³ As reported by Singh *et.al*,²⁰ hydrazine hydrate is a eco-friendly material, which contains a large amount of H₂ (7.9 wt%) and can be easily decompose to H₂ and N₂ at RT with RhNPs. However, to the best of our knowledge, no catalyst that catalyse the reduction of nitroarenes to aminoarenes with hydrazine hydrate at room temperature in aqueous medium with 100% yields at the TOF of > 6000 h⁻¹ is reported. Hence, herein, the stabilization of RhNPs on SBA-NH₂ (RhNPs/SBA-NH₂), its characterization and breakthrough catalytic activity including reusability has been described.

Results and Discussion

The structural aspects of RhNPs/SBA-NH₂ catalyst were investigated by X-ray diffraction analysis. As manifested in Figure 1, three well-resolved reflections of (100), (110) and (200) could be clearly indexed in the hexagonal space group of *p6mm*, exhibiting the well defined and ordered pore structure for SBA-15, SBA-NH₂ and RhNPs/SBA-NH₂ samples.

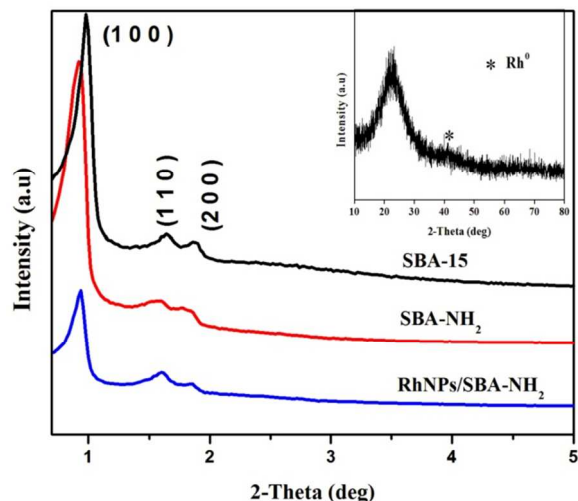


Figure 1 XRD patterns of SBA-15, SBA-NH₂ and RhNPs/SBA-NH₂ catalysts

As inset in Fig. 1, XRD pattern obtained for RhNPs/SBA-NH₂ catalyst in the wide-angle region is displayed, which shows the characteristic reflection (111) plane of metallic rhodium according to card no. JCPDS 87-0714. It is important to note that the diffraction peak of RhNPs/SBA-NH₂ catalyst is very broad and weak, suggesting the existence of very small crystalline RhNPs on the surface of SBA-NH₂. The absence of large and intense diffraction peaks at higher angles further confirms the existence of smaller metallic nanoparticles on SBA-15 support as reported in the literature.²⁴

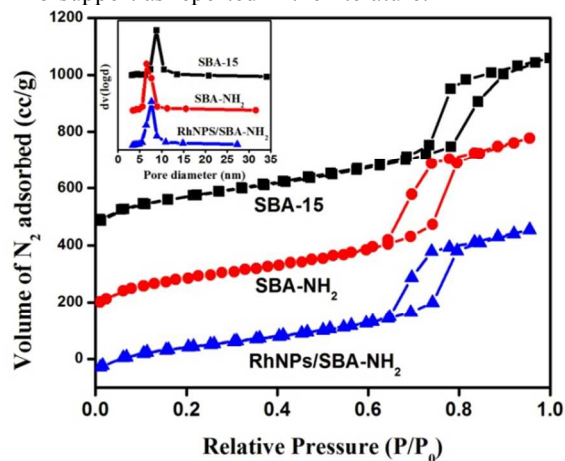


Figure 2 N₂ adsorption-desorption isotherms and pore size distribution curves (inset) of samples

Figure 2 shows the N₂ adsorption-desorption isotherms and pore size distribution curves (inset) of SBA-15, SBA-NH₂ and RhNPs/SBA-NH₂. These isotherms could be classified as type IV characteristic of mesoporous materials. SBA-15, SBA-NH₂ and RhNPs/SBA-NH₂ are uniform in size, which is indicated by the sharp increase in the amount of N₂ adsorbed. The pore size

distributions of the samples (inset in Fig.2), calculated from the N₂ adsorption isotherm following the Barrett–Joyner–Halenda (BJH) method, revealing the narrow pore distribution in the range of 5–10 nm.

As shown in Table 1, the gradual decrease in BET surface area, total pore volume and BJH pore diameter confirms the functionalization of propylamine and deposition of RhNPs. No substantial variation is observed in the structural parameters like *d* spacing, unit cell length and pore wall thickness, confirming the retention of hexagonally ordered SBA-15 structure both in SBA-NH₂ and RhNPs/SBA-NH₂ catalyst.

Table 1 Textural and structural parameters of SBA-15, SBA-NH₂ and RhNPs/SBA-NH₂ samples obtained from N₂ sorption data and low-angle XRD analysis respectively

Catalyst	S _{BET} ^a m ² /g	V _t ^b cc/g	D ^c nm	d ₁₀₀ ^d nm	a ₀ ^e nm	t ^f nm
SBA-15	699	1.06	6.1	9.1	10.5	4.4
SBA-NH ₂	536	0.99	5.8	9.3	11.1	5.3
RhNPs/SBA-NH ₂	451	0.84	5.8	9.8	11.2	5.4

^a BET surface area, ^b total pore volume, ^c BJH pore diameter, ^d periodicity of SBA-15 derived from low angle XRD, ^e unit cell length ($a_0 = 2d_{100}/\sqrt{3}$), ^f pore wall thickness ($t = a_0 - D$).

Transmission electron microscopic (TEM) images were taken to analyze the distribution of rhodium species and to directly observe the morphology of RhNPs/SBA-NH₂ catalyst. As shown in Figure 3, RhNPs were highly dispersed in the mesopore channels of SBA-NH₂. The size distribution histograms for the catalyst were obtained by manually measuring the particles from TEM image. The RhNPs are distributed in the range of 1.5–3 nm. Similar kind of high and uniform dispersion of PdNPs in the pore channels of SBA-NH₂ were described in one of our recent publications.²⁵

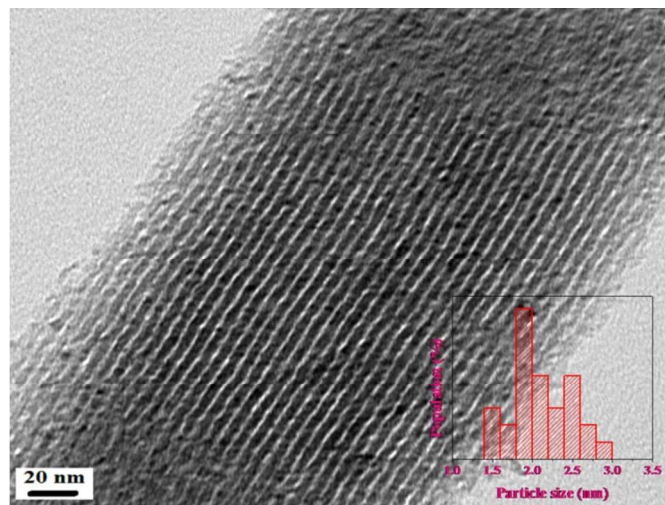


Figure 3: TEM image of RhNPs/SBA-NH₂ catalyst

Figure 4 shows the SEM image of RhNPs/SBA-NH₂, which indicates that the particles are freely distributed and are cylindrical in shape. The EDX shows the amount of Rh is 2.06

wt% in RhNPs/SBA-NH₂ sample.

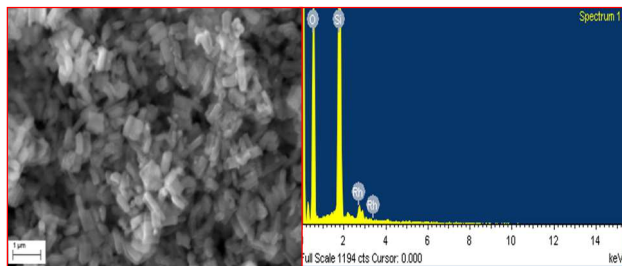


Figure 4 SEM image and its EDAX of RhNPs/SBA-NH₂

XPS spectrum of RhNPs/SBA-NH₂ sample is shown in Figure 5, in which, the 3d_{5/2} and 3d_{3/2} peaks of metallic Rh appear at binding energies 307.7 and 312.8 eV respectively. The XPS results are consistent with the reported literature for the confirmation of zero valent metallic Rh.²⁶

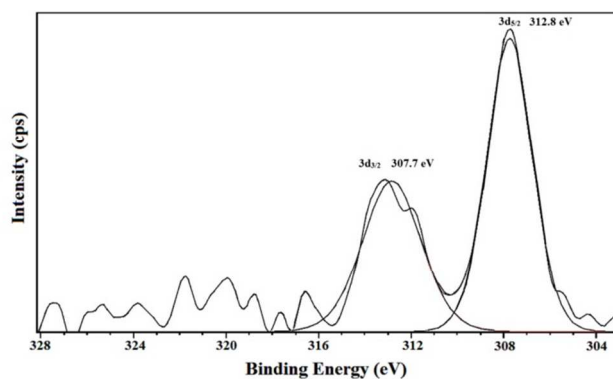


Figure 5 X-ray photoelectron spectrum of RhNPs/SBA-NH₂

Figure 6 shows the FT-IR spectra of SBA-15, SBA-NH₂ and RhNPs/SBA-NH₂, recorded in the region of 4000-400 cm⁻¹.

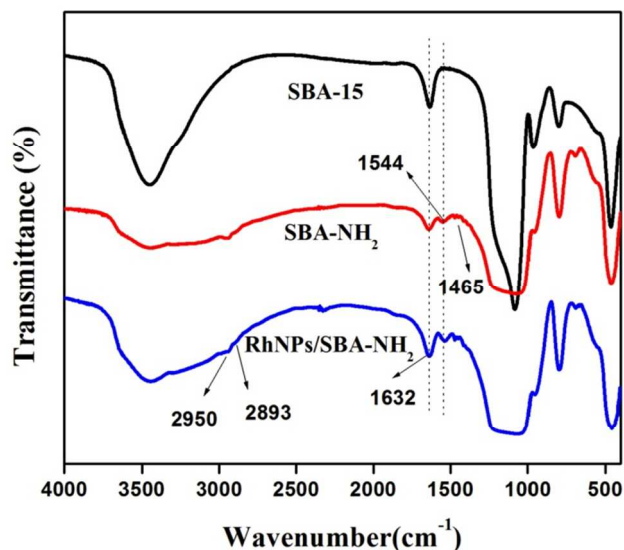
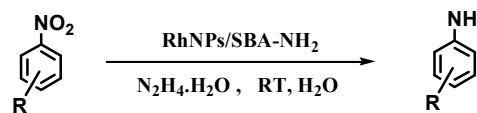


Figure 6 FT-IR spectra of the SBA-15, SBA-NH₂ and RhNPs/SBA-NH₂ samples

As shown in Figure 6, the infrared spectrum of SBA-15 exhibits the typical Si-O lattice vibration in two regions between 1450-900 cm⁻¹ and 900-450 cm⁻¹. Additionally, two bands appear at 3450 cm⁻¹ and 1635 cm⁻¹ due to the O-H stretching and H-O-H (physisorbed water) bending vibrations respectively. Upon amine functionalization, a decrease in the intensity of the bands at 3450, 800 and at 960 cm⁻¹ is observed, indicating the occurrence of reaction between the isolated silanol groups of SBA-15 surface with the methoxy groups of aminopropyl trimethoxy silane. The 2950 and 2893 cm⁻¹ bands in SBA-NH₂ are assigned to ν_{CH} of the -CH₂ groups, and the bands at 1544 and 1465 cm⁻¹ are attributed to δ_{NH} of the -NH₂ groups.²⁷

The catalytic activity of RhNPs/SBA-NH₂ catalyst in the chemoselective hydrogenation of nitroarenes was carried out at room temperature with hydrazine hydrate as hydrogen source in aqueous medium (Scheme 1).



Scheme 1 chemoselective hydrogenation of nitroarenes to aminoarenes

Nitrobenzene is used as model substrate in the chemoselective hydrogenation reaction. Different experiments were conducted using nitrobenzene as a substrate with SBA-15, SBA-NH₂ and without catalyst. No substantial amount of nitrobenzene conversions were obtained with the use of parent SBA-15, SBA-NH₂ and without catalyst (Table 2, entries 1-3), confirming the need for a metal to decompose the hydrazine hydrate and to perform the hydrogenation of nitrobenzene as expected.

Table 2 Hydrogenation of Nitrobenzene with different catalysts

S.No	Catalyst	Conv. (%)	Yield (%)	TOF ^a
1	No catalyst	0	0	-
2	SBA-15	0	0	-
3	SBA-NH ₂	0	0	-
4	RhNPs/SBA-NH ₂	100	99	6117

Nitrobenzene = 1 mmol, catalyst = 10 mg, Hydrazine hydrate = 2 mmol, water = 3 ml, temperature = RT, time = 5 min.

^a TOF = turnover frequency, moles of product/moles of catalyst h⁻¹

Notably, nitrobenzene is completely reduced to aniline with 99% yield (Table 2, entry 4) when RhNPs/SBA-NH₂ used as a catalyst with high Turnover frequency, i.e., 6117 h⁻¹, which is 6 times greater than that of reported TOF of the best catalyst, i.e., rhodium nanoparticles containing porous ionic copolymer (Rh/PICP) catalyst.²¹ Apart from its lower activity compared to the present RhNPs/SBA-NH₂ catalyst, the Rh/PICP catalyst was used at higher temperature (60 °C) with organic solvents (ethanol) instead of RT and water solvent. However, the study²¹ reveals that the supported rhodium nanoparticles as catalyst and hydrazine hydrate as a H₂ source are effective for the chemoselective reduction of nitroarenes to aminoarenes

compared to either noble metal (Pt, Pd, Ru etc..) catalysts or base metal (Ag, Cu, Au etc..) catalysts. The activity of different important catalysts in terms of TOF is presented in Table 4.

Table 3 Efficiency of various reported catalysts including present RhNPs/SBA-NH₂ catalyst

Catalyst	Solvent	H ₂ source	T/°C	TOF/h	Ref.
RhNPs/SBA	Water	N ₂ H ₄ .H ₂ O	RT	6117	P
NAP-Mg-Au ⁰	Water	NaBH ₄	RT	1.8	22
Rh/PICP	Ethanol	N ₂ H ₄ .H ₂ O	60	990	21
Rh/Fe ₃ O ₄	Ethanol	N ₂ H ₄ .H ₂ O	80	103	10
AuNPs magn.	Ethanol	TMDS	RT	95	11a
Au/TiO ₂ -VS	CO/H ₂ O	EtOH/H ₂ O	RT	99	11i
Pt nanowires	Xylene	H ₂	80	57	8h
Fe(OAc) ₂	THF	N ₂ H ₄ .H ₂ O	100	3.33	19a
Pd/CF	Ethanol	H ₂	35	307	7e
Fe(acac) ₂	THF	TMDS	60	0.42	19b
ReIO ₂ (PPh ₃) ₂	Toluene	PhMe ₂ SiH	110	0.79	19c
NAP-Mg-Pd ⁰	THF	H ₂	RT	33	7f

P = present work

Table 3 demonstrate that the present RhNPs/SBA-NH₂ catalyst is far more active in the chemoselective reduction of nitroarenes to aminoarenes under mild reaction conditions in green water medium. The cutting-edge feature of this catalyst is its high activity, which arises from its structural and textural features including isolated distribution of tiny nanoparticles of rhodium in the mesopore channels of SBA-NH₂, which acts as multi-tubular reactor in diffusion-free environment. As discussed in the preceding sections, similar to that of SBA-15, hexagonally ordered mesopore channels exists in SBA-NH₂ support. Most of the RhNPs prefer to occupy the internal pore channels of SBA-NH₂ support rather than its external pore surface due to usage of hydrophobic solvent²⁹ during the deposition of RhNPs. Isolated dispersion of RhNPs occurs in the pore channels rather than agglomeration due to confinement effect and electrostatic interaction of amine functional groups. The RhNPs located in the mesopore channels of SBA-NH₂ are highly accessible to the reactant molecules while passing through the channels during the course of reaction. In other words, the RhNPs containing mesopore channels are nothing but multi-tubular reactors during the reaction.

In conventional hydrogenation reactions large excess of H₂ will be supplied through external source, whereas in the present process the required H₂ necessarily be generated. i.e., the decomposition of hydrazine necessarily occurred according to equation (i) before the commencement of nitroarenes hydrogenation. It is important to note that the present RhNPs/SBA-NH₂ catalyst is capable of catalyzing both the

decomposition of hydrazine and hydrogenation of nitroarenes simultaneously under mild reaction conditions (1 atm. pressure and room temperature) in aqueous medium with 100% conversion in 5 min.

In order to investigate the scope of the reaction with the presented catalyst system, various functionalized nitro arenes were subjected to hydrogenation with RhNPs/SBA-NH₂ catalyst under similar reaction conditions. The results are summarized in Table 4, which shows that RhNPs/SBA-NH₂ was highly active and extremely selective for the hydrogenation of all substrates without disturbing other functional groups, indicating a high versatility of the catalyst.

Table 4 Selective hydrogenation of various nitro arenes catalysed by RhNPs/SBA-NH₂ catalyst

S.No	Substrate	Product	Conversion (%)	TOF (h ⁻¹)
1			100	6117
2			100	6117
3			100	6117
4			100	3059
5			100	3059
6			100	3059
7			100	3059
8			100	3059
9			100	3059
10			100	3059
11			100	2039
12			100	2039

Substrate = 1 mmol, catalyst = 10 mg, Hydrazine hydrate = 2 mmol, water = 3 ml, temperature = RT

In order to understand the process of reaction either through heterogeneous or homogeneous, a hot filtration test was carried out with little modification. In general, the hot filtration tests are being conducted at about 50% conversion levels, but in the present study reaction time is too short to conduct the hot filtration test. In the present study, after completion of the

reaction, the catalyst was separated from the reaction mixture by a simple filtration. To the filtrate, nitrobenzene and hydrazine hydrate were added and run the reaction without adding catalyst for 3 h and analyzed by GC. No significant increase in conversion was observed, revealing the reduction of nitrobenzene is proceeds in heterogeneous manner and the filtrate was analyzed by ICP-AES for the estimation of Rh, but no Rh species was detected in the filtrate, revealing the absence of Rh leaching or below the detection limit of the instrument (<7 ppb).

To verify the scale up study, reactants and catalyst were taken 10 times higher and found extremely high turnover frequency of 6116 h^{-1} with 100% selectivity of aniline.

The recyclability of the RhNPs/SBA-NH₂ sample was examined in the chemoselective hydrogenation of nitrobenzene under the similar conditions and displayed in Figure 7. After the catalytic reaction, the catalyst was isolated from the liquid phase by centrifugation, thoroughly washed with methanol, and then reutilized as catalyst in subsequent runs under identical reaction conditions. The results included in Fig. 7 indicate that no efficiency loss was observed in the hydrogenation of nitrobenzene for up to six runs. The study reveals that the Rh nanoparticles are well stabilized and are uniformly distributed on amine functionalized SBA-15 due to SBA-NH₂ pore confinement effect and NH₂ stabilizing nature, which can be explained that the holes formed in the d-band of metal interacts with the lone pair electrons of amine functional group.³⁰

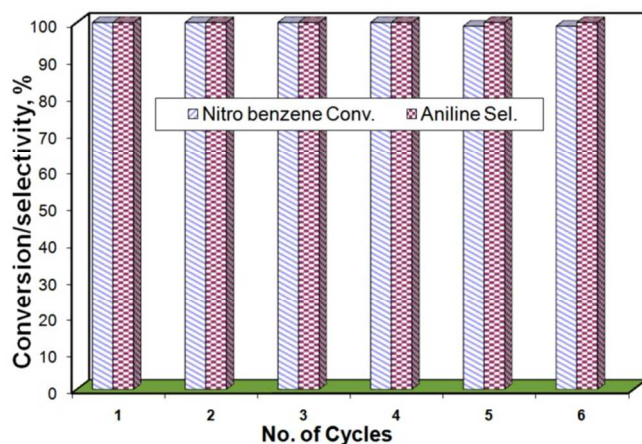


Figure 7 Recyclability of RhNPs/SBA-NH₂ catalyst

Experimental

Preparation of Catalyst: The siliceous SBA-15 was synthesized by using P123 as template and TEOS as silica source in accordance with the literature procedures³¹. In a typical synthesis, a solution of EO₂₀PO₇₀EO₂₀:2M HCl: TEOS: H₂O = 2:60:4.25:15 (mass ratio) was prepared, stirred for 24 h at 40 °C and then hydrothermally treated at 100 °C under static condition for 24 h, subsequently filtered, dried at 100 °C and calcined at 550 °C for 8 h, to yield mesoporous silica SBA-15.

SBA-NH₂ was synthesized accordance with our previous publication.²⁵ Aminopropyl triethoxy silane (APTES) (3 mL) was added drop wise to a suspension of SBA-15 (1g) in dry toluene (30 mL), under N₂ atmosphere. The resulting mixture was refluxed for 24 h. After that, the suspension was filtered and washed thoroughly with toluene and ethanol. The resulting solid was dried under

vacuum at room temperature and labeled as SBA-NH₂. The amount of nitrogen obtained from CHN elemental analysis is 1.5 mmol g^{-1} .

RhNPs were prepared by using hydrophobic dichloromethane solvent as transport medium to inject rhodium precursor into the pores of modified SBA-15. In a typical procedure, requisite amount of rhodium acetyl acetone was dissolved in dry dichloromethane solvent, to this SBA-NH₂ was added and stirred at room temperature and solvent was evaporated. The resulting solid was dried at room temperature for 12 h. Solid catalyst was reduced with NaBH₄ in isopropanol, filtered and washed thoroughly with water and methanol, denoted as RhNPs/SBA-NH₂.

Characterization of catalysts: The X-ray diffraction (XRD) patterns were recorded at room temperature using an X-ray diffractometer (Multiflex, M/s. Rigaku, Japan) with a nickel filtered CuK α radiation. N₂ adsorption-desorption isotherms were recorded on a N₂ adsorption unit at at-196 °C (Quadrasorb-SI V 5.06, M/s. Quantachrome Instruments Corporation, USA). The samples were out-gassed at 200 °C for 4 h before the measurement. Transmission electron microscope (TEM) analysis was made using a FEI Technai G2 S-Twin Serial Number D 2083 at an accelerating voltage of 200 kV. The XPS analysis was made on a photoelectron spectrometer (KRATOS Axis 165, Shimadzu, Japan) with Mg K α radiation (1253.6 eV). Rh contents of the sample were analysed with a simultaneous ICP-AES allied analytical system (Perkin Elmer 3100XL). The FT-IR spectra of the materials were recorded on a Perkin-Elmer FT-IR spectrometer at ambient conditions using KBr discs with a nominal resolution of 4 cm^{-1} and averaging 5 spectra.

Catalytic activity: The catalytic activity of RhNPs /SBA-NH₂ in chemoselective hydrogenation of nitro arenes has been carried out in the liquid phase at room temperature. In a typical procedure 1 mmol of reactant, 2 mmol of hydrazine hydrate and 10 mg of catalyst in 3 ml water were added to a 10 ml RB flask and stirred at room temperature. After completion the products were extracted with ethyl acetate and the catalyst was removed by centrifugation. The product analysis was made by GC-MS (QP-5050 model, M/s. Shimadzu Instruments, Japan) equipped with equity-1 capillary column (0.32 mm dia. and 25 m long, supplied by M/s. J & W Scientific, USA).

Conclusion

In summary, an efficient and green RhNPs/SBA-NH₂ solid catalyst has been developed with particle size of 1-3 nm for aqueous medium chemoselective hydrogenation of nitroarenes to corresponding aminoarenes at room temperature with short reaction times in excellent yields. Apart from its high activity and chemoselectivity, ease of separation, reusability, facile preparation are its meritorious features.

Acknowledgements

Saidulu and Ravi kumar acknowledge CSIR, and Siva Sankar acknowledge UGC, New Delhi, for research fellowship.

Notes and references

Catalysis Laboratory, Indian Institute of Chemical Technology, Hyderabad-500607, India. Fax: +91-40-27160921; Tel: +91-40-27193232; E-mail: david@iict.res.in

Electronic Supplementary Information (ESI) available: [details of any supplementary information available should be included here]. See DOI: 10.1039/b000000x/

‡ Footnotes should appear here. These might include comments relevant to but not central to the matter under discussion, limited experimental and spectral data, and crystallographic data.

- 1 H. U. Blaser, *Scienc*, 2006, **313**, 312; A. Corma, P. Concepcion, P. Serna, *Angew. Chem. Int. Ed.*, 2007, **46**, 7266; X. Meng, H. Cheng, Y. Akiyama, Y. Hao, W. Qiao, Y. Yu, F. Zhao, S. I. Fujita, M. Arai, *J. Catal.*, 2009, **264**, 1.
- 2 S. U. Sonavane, M. B. Gawande, S. S. Deshpande, A. Venkataraman and R. V. Jayaram, *Catal. Commun.*, 2007, **8**, 1803; X. Yuan, N. Yan, C. Xiao, C. Li, Z. Fei, Z. Cai, Y. Kou and P. J. Dyson, *Green Chem.*, 2010, **12**, 228.
- 3 M. Takasaki, Y. Motoyama, K. Higashi, S. H. Yoon, I. Mochida and H. Nagashima, *Org. Lett.*, 2008, **10**, 1601.
- 4 F. Wang, J. Liu and X. Xu, *Chem. Commun.*, 2008, 2040; A. Corma, P. Serna, P. Concepción and J. J. Calvino, *J. Am. Chem. Soc.*, 2008, **130**, 8748.
- 5 A. Woźniwodzka, G. Gołuński, and J. Piosik, *ISRN Biophysics*, 2013, doi.org/10.1155/2013/740821.
- 6 T. Sugimura, K. Wakabayashi, H. Nakagama, and M. Nagao, *Cancer Science*, 2004, **95**, 290.
- 7 (a) J. Lipowitz and S. A. Bowman, *J. Org. Chem.*, 1973, **38**, 162; (b) R. J. Rahaim, Jr. and R. E. Maleczka, *Org. Lett.*, 2005, **7**, 5087; (c) R. J. Rahaim, Jr. and R. E. Maleczka, Jr., *Synthesis*, 2006, 3316; (d) S. Srinivasan and X. Huang, *Chirality*, 2008, **20**, 265–277; (e) H. Wu, L. Zhuo, Q. He, X. Liao and B. Shi, *Applied Catalysis A: General*, 2009, **366**, 44; (f) M. L. Kantam, R. Chakravarti, U. Pal, B. Sreedhar and S. Bhargava, *Adv. Synth. Catal.*, 2008, **350**, 822.
- 8 (a) K. A. Andrianov, V. I. Sidorov and M. I. Filimonova, *Zh. Obshch. Khim.*, 1977, **47**, 485; (b) X. Lin, M. Wu, D. Wu, S. Kuga, T. Endoe and Y. Huang, *Green Chem.*, 2011, **13**, 283; (c) V. Pandarus, R. Ciriminna, F. Beland and M. Pagliaro, *Adv. Synth. Catal.*, 2011, **353**, 1306; (d) M. Li, L. Hu, X. Cao, H. Hong, J. Lu and H. Gu, *Chem.–Eur. J.*, 2011, **17**, 2763; (e) Z. Sun, Y. Zhao, Y. Xie, R. Tao, H. Zhang, C. Huang and Z. Liu, *Green Chem.*, 2010, **12**, 1007; (f) M. Takasaki, Y. Motoyama, K. Higashi, S. H. Yoon, I. Mochida and H. Nagashima, *Org. Lett.*, 2008, **10**, 1601; (g) P. Maity, S. Basu, S. Bhaduri and G. K. Lahiri, *Adv. Synth. Catal.*, 2007, **349**, 1955; (h) L. Hu, X. Cao, L. Chen, J. Zheng, J. Lu, X. Sun and H. Gu, *Chem. Commun.*, 2012, **48**, 3445.
- 9 (a) S. Zhao, H. Liang and Y. Zhou, *Catal. Commun.*, 2007, **8**, 1305; (b) K. V. R. Chary and C. S. Srikanth, *Catal. Lett.*, 2009, **128**, 164.
- 10 Y. Jang, S. Kim, S. W. Jun, B. H. Kim, S. Hwang, I. K. Song, B. M. Kim and T. Hyeon, *Chem. Commun.*, 2011, **47**, 3601.
- 11 (a) S. Park, I. S. Lee and J. Park, *Org. Biomol. Chem.*, 2013, **11**, 395; (b) Y. Choi, H. S. Bae, E. Seo, S. Jang, K. H. Park and B.-S. Kim, *J. Mater. Chem.*, 2011, **21**, 15431; (c) Y. Zhang, S. Liu, W. Lu, L. Wang, J. Tian and X. Sun, *Catal. Sci. Technol.*, 2011, **1**, 1142; (d) S. Saha, A. Pal, S. Kundu, S. Basu and T. Pal, *Langmuir*, 2010, **26**, 2885; (e) K. Hayakawa, T. Yoshimura and K. Esumi, *Langmuir*, 2003, **19**, 5517; (f) X. Huang, X. Liao and B. Shi, *Green Chem.*, 2011, **13**, 2801; (g) N. Pradhan, A. Pal and T. Pal, *Langmuir*, 2001, **17**, 1800; (h) X. Bai, Y. Gao, H.-g. Liu and L. Zheng, *J. Phys. Chem. C*, 2009, **113**, 17730; (i) L. He, L.-C. Wang, H. Sun, J. Ni, Y. Cao, H.-Y. He and K.-N. Fan, *Angew. Chem., Int. Ed.*, 2009, **48**, 9538; (j) X.-B. Lou, L. He, Y. Qian, Y.-M. Liu, Y. Cao and K.-N. Fan, *Adv. Synth. Catal.*, 2011, **353**, 281; (k) Y. Chen, J. Qiu, X. Wang and J. Xiu, *J. Catal.*, 2006, **242**, 227.
- 12 (a) A. Chanda, V. V. Fokin, *Chem. Rev.*, 2009, **109**, 725; (b) Minakata, M. Komatsu, *Chem. Rev.*, 2009, **109**, 711; (c) M. Raj, V. K. Singh, *Chem. Commun.*, 2009, 6687.
- 13 (a) J. Paradowska, M. Stodulski, J. Mlynarski, *Angew. Chem.*, 2009, **48**, 4288; (b) M. L. Deb and P. J. Bhuyan, *Tetrahedron Lett.*, 2005, 6453.
- 14 (a) S. Narayan, J. Muldoon, M. G. Finn, V. V. Fokin, H. C. Kolb, K. B. Sharpless, *Angew. Chem., Int. Ed.* 2005, **44**, 3275; (b) A. Manna and A. Kumar, *J. Phys. Chem. A*, 2013, **117**, 2446.
- 15 H. X. Li, F. Zhang, Y. Wan and Y. F. Lu, *J. Phys. Chem. B*, 2006, **110**, 22942.
- 16 D. Y. Zhao, J. L. Feng, Q. S. Huo, N. Melosh, G. H. Fredrickson, B. F. Chmelka and G. D. Stucky, *Science*, 1998, **279**, 548.
- 17 P. P. Sarmah and D. K. Dutta, *Green Chem.*, 2012, **14**, 1086.
- 18 (a) V. S. Kumar, S. S. Reddy, A. H. Padmasri, D. R. Burri, I. A. Reddy, K. S. Rama Rao, *Catal Commun.*, 2007, **8**, 899; (b) B. M. Nagaraja, A. H. Padmasri, P. S. Ramulu, K. H. P. Reddy, D. R. Burri, K. S. Rama Rao, *J. Mol. Catal. A Chem.*, 2007, **278**, 29 3; (c) K. H. P. Reddy, R. Rahul, S. S. Reddy, D. R. Burri, K. S. Rama Rao, *Catal Commun.*, 2009, **10**, 879; (d) B. M. Nagaraja, A. H. Padmasri, D. R. Burri, K. S. Rama Rao, *Int J Hyd Energy*, 2011, **36**, 3417; (e) H. Y. Zheng, Y. L. Zhu, Z. Q. Bai, L. Huang, H. W. Xiang, Y. W. Li, *Green Chem*, 2006, **8**, 107; (f) Y. L. Zhu, H. W. Xiang, G. S. Wu, L. Bai, Y. W. Li, *Chem Commun.*, 2002, **3**, 254; (g) C. V. Pramod, V. Mohan, D. R. Burri, K. S. Rama Rao, *Catal Lett.*, 2013, **143**, 432; (h) C. V. Pramod, M. Suresh, V. Mohan, B. Sridevi, D. R. Burri and K.S. Rama Rao, *Current Catalysis*, 2012, **1**, 140.
- 19 (a) R. V. Jagadeesh, G. Wienhofer, F. A. Westerhaus, A.-E. Surkus, M.-M. Pohl, H. Junge, K. Junge and M. Beller, *Chem. Commun.*, 2011, **47**, 10972; (b) L. Pehlivan, E. Métay, S. Laval, W. Dayoub, P. Demonchaux, G. Mignani and M. Lemaire, *Tetrahedron*, 2011, **67**, 1971; (c) R. G. de Noronha, C. C. Ramao, and A. C. Fernandes, *J. Org. Chem.*, 2009, **74**, 6960.
- 20 (a) S. K. Singh and Q. Xu, *J. Am. Chem. Soc.*, 2009, **131**, 18032; (b) S. K. Singh, X. B. Zhang and Q. Xu, *J. Am. Chem. Soc.*, 2009, **131**, 9894.
- 21 P. Luo, K. Xu, R. Zhang, L. Huang, J. Wang, W. Xing and J. Huang, *Catal. Sci. Technol.*, 2012, **2**, 301.
- 22 K. Layek, M. L. Kantam, M. Shirai, D. N. Hamane, T. Sasaki and H. Maheswaran, *Green Chem.*, 2012, **14**, 3164.
- 23 Y. Gao, D. Ma, C. Wang, J. Guan and X. Bao, *Chem. Commun.*, 2011, **47**, 2432.
- 24 K. K. R. Datta, B. V. S. Reddy, K. Ariga and A. Vinu, *Angew. Chem. Int. Ed.*, 2010, **49**, 5961.
- 25 G. Saidulu, M. Suresh, N. C. K. Prasad, K. S. Rama Rao and D. R. Burri, *RSC Adv.*, 2013, **3**, 11533.
- 26 (a) B. V. Crist, *Handbook of Monochromatic XPS Spectra*, Wiley: Chichester/New York, 2000; (b) Y. W. Zhang, M. E. Grass, S. E. Habas, F. Tao, T. F. Zhang, P. D. Yang, G. A. Somorjai, *J. Phys. Chem. C*, 2007, **111**, 12243; (c) H. B. Pan and C. M. Wai, *J. Phys. Chem. C*, 2009, **113**, 19782.
- 27 P. Wang, Q. Lu and J. Li, *Material Research Bulletin*, 2010, **45**, 129.
- 28 (a) Y. Chen, C. Wang, H. Liu, J. Qiu and X. Bao, *Chem. Commun.*, 2005, 5298; (b) K. I. Shimizu, Y. Miyamoto and A. Satsuma, *J. Catal.*, 2010, **270**, 86; (c) S. Diao, W. Qian, G. Luo, F. Wei and Y. Wang, *Appl. Catal., A*, 2005, **286**, 30; (d) U. Sharma, P. Kumar, N. Kumar, V. Kumar and B. Singh, *Adv. Synth. Catal.*, 2010, **352**, 1834; (e) A. Sama and B. Ranu, *J. Org. Chem.*, 2008, **73**, 6867.
- 29 (a) M. I. Clerc, D. Bazin, M. D. Appay, P. Beauvier and A. Davidson, *Chem. Mater.*, 2004, **16**, 1813; (b) I. Lopes, N. El Hassan, H. Guerber, G. Wallez and A. Davidson, *Chem. Mater.*, 2006, **18**, 5826; (c) Q. S. Lu, Z. Y. Wang, J. G. Li, P. Y. Wang and X. L. Ye, *Nanoscale Res. Lett.*, 2009, **4**, 646; (d) L. Tian, Q. Yang, Z. Jiang, Y. Zhu, Y. Pei, M. Qiao and K. Fan, *Chem. Commun.*, 2011, **47**, 6168.

- 30 C. K. P. Neeli, G. Saidulu, V. S. P. Ganjala, R. S. Kamaraju and D. R. Burri, *RSC Adv.*, 2014, DOI: 10.1039/C4RA00791C.
- 31 D. Zhao, J. Feng, Q. Huo, N. Melosh, G. H. Fredrickson, B. F. Chmelka and G. D. Stucky, *Science*, 1998, **279**, 548; G. Saidulu, B. Padma, V. Venkateswarlu, K. S. Rama Rao and D. R. Burri, *Catal. Sci. Technol.*, 2013, **3**, 409; G. Saidulu, N. Anand, K. S. Rama Rao, A. Burri, S. E. Park and D. R. Burri, *Catal. Lett.* 2011, **141**, 1865.